

# A modal approach for the solution of the non-linear induction problem in ferromagnetic media

Anastassios Skarlatos and Theodoros Theodoulidis, *Senior Member, IEEE*

**Abstract**—The non-linear induction problem in ferromagnetic media is solved using the fixed-point iteration method, where the linearized problem at each iteration is treated by means of a modal approach. The proposed approach does not require meshing of the solution domain, which results in fast computations comparing to conventional mesh-based numerical techniques. Both harmonic and pulse excitations are considered via Fourier and Laplace transform, respectively. An efficient method for the fast computation of the inverse Laplace transform of the magnetic polarization signals is also devised based on the generalized pencil-of-function (GPOF) method. Although being restricted to one dimensional configurations, the present work provide the tools for the treatment of two and three dimensional problems, whose study is under way.

## I. INTRODUCTION

The solution of the induction problem in configurations involving ferromagnetic media, is in general case a non-linear problem. For relatively weak fields, linearization provides a very good approximation of the real solution. This is for example the case in classical eddy-current testing (ECT) or wave propagation applications. Nonetheless, when excitation currents of medium or high intensity are involved, the full non-linear formulation has to be considered. Such currents are encountered in electric machines and transformers as well as in material evaluation applications, just to mention some of the most pertinent practical situations.

The general way of addressing a non-linear field problem can be roughly sketched as follows: construct a sequence of successive approximations to the solution by treating a linearized problem each time, and iterate until a convergence criterion is satisfied. There are principally two main approaches for establishing the above iterative scheme; either by expressing the non-linear formulation in terms of a fixed-point problem, that is by constructing the sequence  $\mathbf{x}^{(l+1)} = \mathcal{G}\mathbf{x}^{(l)}$ , or by reformulating it as an homogeneous equation  $\mathcal{F}\mathbf{x} = 0$  and searching its roots using the Newton-Raphson method, i.e. via the relation  $\mathbf{x}^{(l+1)} = \mathbf{x}^{(l)} - [d\mathcal{F}/d\mathbf{x}^{(l)}]^{-1} \mathcal{F}\mathbf{x}^{(l)}$ . Both methods have pros and cons regarding their stability and their convergence speed, and various techniques based on the introduction of relaxation conditions as well as hybridization of the two approaches have been proposed for achieving optimal performance [1].

Considerable effort has been given during the past years in applying both iterative schemes for treating the electro-magnetic induction problem in ferromagnetic media, where the linearized problem at each iteration is solved by means

of a numerical technique. In most cases, the finite elements method (FEM) is the numerical tool of choice [2], [3], yet numerous works using other mesh-based approaches like the finite integration technique (FIT) [4] or the integral equation approach [5], [6] exist as well. The relative literature is vast, and the above list of references tends only to be indicative.

The application of analytical methods for the solution of the non-linear field problem is by far less studied, to the best of the authors knowledge. This trend may be explained by the difficulty of the problem, and the limited number of cases that can be tackled using analytical approaches in comparison with the existing versatile numerical tools. Yet, a few attempts to address simple geometries, usually by resorting to (sometimes coarse) approximations, can be found in the literature. Such attempts comprise the approximation of the abrupt magnetic transition approximation, initially proposed by Wolman and Kaden [7] and further worked in later articles [8], [9], or the treatment of the eddy-current problem in a ferromagnetic rod excited by a long solenoid by means of a perturbation approach as is proposed by Nayfeh and Asfar in [10]. The cartesian counterpart of the latter problem, namely an infinite plate with uniform current layers on both sides is treated by Labridis and Dokopoulos in [11] by performing successive approximations to the magnetic permeability in the diffusion equation.

An alternative strategy to such ad hoc approaches with limited domain of validity, would be to apply a modal-based approach for the inversion of the linearized problem occurring at each iteration of the general iterative techniques mentioned above. Modal techniques have proved to be a very powerful tool, which allowed the treatment of a number of important linear eddy-current problems [12]–[16]. The interest in applying modal methods, relies on the shorter calculation times with respect to the numerical techniques, the absence of the computational grid as well as the better insight to the physics of the problem they provide.

The inherit difficulty in treating inhomogeneous materials using modal techniques, makes their use with Newton-Raphson like schemes, where the Jacobian of the material law is involved, complicated. This restriction, however, does not occur when considering fixed-point schemata which leave the material properties of the linerized problem intact. This in conjunction with its good stability properties makes the fixed point approach the method of choice in this work.

The main purpose of this article is to explore the construction of such semi-analytical based solutions to the non-linear induction problem. Since it is a first attempt, the focus in this article will lie on setting up a solving strategy with regard to two rather academic problems, namely a one-dimensional coil with a ferromagnetic core in the cartesian and the cylindrical

A. Skarlatos is with the CEA, LIST, F-91191 Gif-sur-Yvette cedex, France.

T. Theodoulidis is with the Department of Mechanical Engineering, University of Western Macedonia, Bakola & Sialvera, 50100 Kozani, Greece.

systems. Yet, despite being of very simple geometry, these problems still present a practical interest, since the herein developed solutions may deliver some useful approximations for configurations met in engineering problems like yokes and coil cores.

Both harmonic and pulsed excitations will be considered in the context of this work. The discrete spectrum of the former makes the frequency domain formulation in combination with Fourier synthesis the most straight-forward and, in the same time, efficient approach [3], [6]. In the latter case, the direct treatment in time domain seems to be more relevant. Following previous works, the analysis is facilitated by formulating the problem in the Laplace domain [17], [18]. A considerable difficulty when working in the Laplace domain is the inverse transformation of arbitrary signals back into the time domain. Instead of adopting a numerical inversion, an alternative approach is proposed based on the generalized pencil-of-function (GPOF) method [19], [20]. According to the GPOF method, an arbitrary signal can be approximated in the Laplace domain by a sum of rational functions, whose inverse transformation back into the time domain exist in closed form.

Work is under way for the extension of the herein developed ideas to two dimensional configurations, in order to tackle more realistic configurations involving cylindrical coils around bars or above ferromagnetic plates.

## II. FORMAL SOLUTION USING THE FIXED-POINT METHOD

The magnetic constitutive relation of a ferromagnetic material reads:

$$\mathbf{B} = \mu_0[\mathbf{H} + \mathbf{M}(\mathbf{H})] \quad (1)$$

where  $\mu_0$  is the magnetic permeability of the free space, and  $\mathbf{M}$  stands for the magnetization of the material, which comprises the non-linear effects. An equivalent, in some cases more useful form of (1), is obtained by introducing the magnetic polarization  $\mathbf{I} := \mu_0\mathbf{M}$ . Equation (1) becomes then

$$\mathbf{B} = \mu_0\mathbf{H} + \mathbf{I}(\mathbf{H}). \quad (2)$$

The last equation can be written formally as follows

$$\mathbf{I}(\mathbf{B}) = \mathbf{B} - \mu_0\mathbf{H}(\mathbf{B}) \quad (3)$$

where  $\mathbf{H}(\mathbf{B})$  is the inverse material curve in the  $\mathbf{H} - \mathbf{B}$  plane, which for the purposes of our analysis will be considered known.

For reasons that will be explained below, it is interesting to consider a magnetic permeability different than that of the free space, i.e.  $\mu > \mu_0$ . The magnetic polarization in (2) and (3) then should be replaced by an effective one, namely  $\mathbf{I} \rightarrow \mathbf{I}' + (\mu - \mu_0)\mathbf{H}$ . Notice that,  $\mathbf{I}'$  in contrast with the original variable  $\mathbf{I}$ , does not represent a physical quantity any more; it is merely introduced for mathematical convenience. Once  $\mathbf{I}'$  defined, the prime symbol will be dropped henceforth, i.e. the use of the effective magnetic polarization will be implied from this point forward.

Using (3) and applying the quasi-static approximation, the diffusion equation for the magnetic field in the magnetic medium becomes

$$\nabla \times \nabla \times \mathbf{B} + \mu\sigma \frac{\partial \mathbf{B}}{\partial t} = \nabla \times \nabla \times \mathbf{I}(\mathbf{B}). \quad (4)$$

Taking into account  $\nabla \cdot \mathbf{B} = 0$ , and making the plausible assumption of the absence of free magnetic poles in the bulk material ( $\nabla \cdot \mathbf{I} = 0$ )<sup>1</sup>, (4) reduces to

$$\nabla^2 \mathbf{B} - \mu\sigma \frac{\partial \mathbf{B}}{\partial t} = \nabla^2 \mathbf{I}(\mathbf{B}). \quad (5)$$

Let us set  $\mathcal{D} := \nabla^2 - \mu\sigma \partial/\partial t$ , the diffusion operator. According to Banach fixed point theorem, if the non-linear operator  $\mathcal{D}^{-1}\nabla^2 \mathbf{I}$  is a contraction, then the sequence

$$\mathbf{B}^{(l+1)} = \mathcal{D}^{-1}\nabla^2 \mathbf{I}[\mathbf{B}^{(l)}] \quad (6)$$

converges to the fixed-point of the operator, which is also the solution of (5). The condition for the convergence of (6) is that the magnetization curve is Lipschitzian and monotonous, as it has been shown by Hăntilă in [21]. This condition is met by the sigmoid B-H curves of the most important ferromagnetic media for  $\mu < 2\mu_{min}$ ,  $\mu_{min}$  being the minimum of the differential permeability. The closer the value of  $\mu$  to the upper limit, the better the contraction factor, which justifies our interest to work with the effective magnetic polarization introduced above. Practically, the choice of  $\mu$  is a compromise between convergence speed and stability of the algorithm. For the rest of the article, the convergence will be considered as guaranteed without further investigation.

The general iterative algorithm for the solution of the non-linear equation using the fixed-point theorem, an approach referred also to in the literature as Picard-Banach or polarization method, is summarized schematically by the following pseudo-code

```
Set  $\mathbf{I}^{(0)}, \Delta \mathbf{I}^{(0)}$ 
for  $l = 0, 1, \dots$  until  $\|\Delta \mathbf{I}^{(l)}\| < \epsilon$ 
  Solve  $\mathbf{B}^{(l+1)} = \mathcal{D}^{-1}\nabla^2 \mathbf{I}^{(l)}$ 
  Evaluate  $\mathbf{I}^{(l+1)} = \mathbf{B}^{(l+1)} - \mu\mathbf{H}[\mathbf{B}^{(l+1)}]$ 
  Calculate the residual  $\|\Delta \mathbf{I}^{(l+1)}\|$ 
```

The above scheme is generic in the sense that it does not depend on the way that  $\mathcal{D}^{-1}$  is calculated. In the following paragraphs the modal approach will be applied for the solution of (5) for two important piece geometries: infinite plate and cylindrical rod.

## III. 1D CARTESIAN PROBLEM: FERROMAGNETIC PLATE BETWEEN TWO INFINITELY LONG CURRENT LAYERS

We shall begin the study of the non-linear eddy-current problem by considering a ferromagnetic plate of thickness  $d$  sandwiched by two opposite infinite current layers  $\mathcal{K}(t)$ . The geometry of the problem is illustrated in figure 1. Despite its simplicity, this 1D configuration resembles an infinite, transnationally symmetric yoke, and hence the derived solution can be used to approximate the behaviour of realistic 3D yokes.

As it is shown in figure 1, the antisymmetry of the configuration allows the problem to be reformulated in an equivalent one, where the solution is restricted to the non-negative  $z$  semi-axis in combination with a perfectly electric conductor

<sup>1</sup>Notice that this assumption is justified only in the case of homogeneous  $\mu$ .

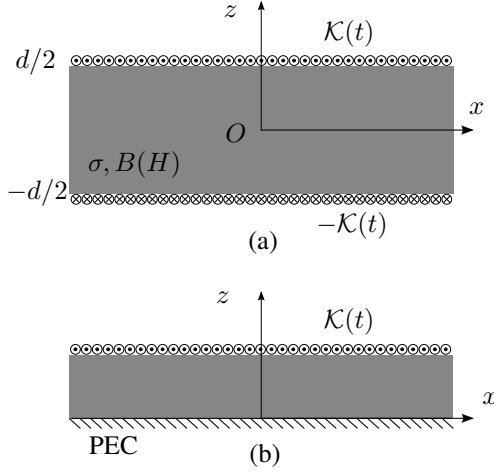


Fig. 1. Infinitely long ferromagnetic plate between two opposite current layers: (a) real configuration and (b) equivalent structure with odd parity.

boundary condition at the  $z = 0$  plane (plane of symmetry). This reformulation results in a simplification of the original problem.

Owing to the symmetry of the configuration, the magnetic field will lie along the  $x$  direction and it will depend only upon the distance from the interface, i.e. it will be  $\mathbf{H} = H(z) \mathbf{e}_x$ , whereas the electric field will be directed along  $y$  and it will be also a function of  $z$ , namely  $\mathbf{E} = E(z) \mathbf{e}_y$ . Consequently, the vector equation (5) reduces to the scalar one

$$\frac{\partial^2 B}{\partial z^2} - \mu\sigma \frac{\partial B}{\partial t} = \frac{\partial^2 I}{\partial z^2}. \quad (7)$$

The magnetic constitutive relation that we need to consider is also scalar, i.e. we can write

$$I(B) = B - \mu H(B). \quad (8)$$

In the following two subsections we shall derive the solution to the one dimensional cartesian problem for the two most interesting types of excitation, namely harmonic and unit step. Other more general forms of excitations like the periodic waveforms (square, triangular etc.) or pulse (with rectangular or exponential profile) can be derived based on the solutions of the basic aforementioned cases. For the analysis of periodic signals the use of the Fourier series is better suited, whereas the Laplace transform is the most efficient tool when studying plused excitations. Hence, the analysis will be adapted to the type of the problem that we are studying in order to use the most efficient approach.

#### A. Harmonic excitation

Let us assume a harmonic current excitation, i.e. let  $K(t) = K_0 \cos(\omega_0 t)$  with  $\omega_0 = 2\pi f_0$  being the angular frequency. Since we are dealing with a non-linear problem the final signals will still be periodic, yet their spectrum will consist by an infinite number of frequencies that are integer multiples of the excitation one  $f_0$ , i.e. it will be  $f_n = n f_0$  with

$n = 1, 2, \dots, \infty^2$ . The magnetic induction can be described by means of a Fourier series, namely

$$B(z, t) = \sum_{n=-\infty}^{n=\infty} B_n(z) e^{i n \omega_0 t} \quad (9)$$

with the series coefficients being given by

$$B_n(z) = \frac{1}{T} \int_0^T B(z, t) e^{-i n \omega_0 t} dt \quad (10)$$

and  $T = 1/f_0$  being the period of the signal. The corresponding expansions for  $H$  and  $I$  are given by the same relations.

The diffusion equation (7) reduces then to the Helmholtz inhomogeneous equation, which for  $n$ -th harmonic reads

$$\frac{d^2 B_n}{dz^2} - k_n^2 B_n = \frac{\partial^2 I_n}{\partial z^2} \quad (11)$$

with  $k_n^2 = i n \omega_0 \mu \sigma = i \omega_n \mu \sigma$ .

Assume now that the magnetic polarization  $I_n$  is known. Then following the standard theory of differential equations, the solution of (11), can be constructed by the superposition of the solution to the homogeneous equation and a partial solution. The former, after taking symmetry of the tangential magnetic field across the  $z = 0$  plane into account proves easily to be

$$B_n^{(h)}(z) = A_n \cosh(k_n z). \quad (12)$$

The expansion coefficient  $A_n$  will be determined by the application of the boundary conditions at  $z = d/2$ .

In order to construct the partial solution of (7), we assume that at a given time instant  $t$ , both the magnetic field and the polarization can be expanded in the eigenfunction-basis of the spatial operator  $\partial^2/\partial z^2$ , i.e.

$$\left\{ \begin{array}{l} I_n(z) \\ B_n^{(p)}(z) \end{array} \right\} = \left\{ \begin{array}{l} C_{n,0} \\ D_{n,0} \end{array} \right\} + \sum_{i=1}^{\infty} \left\{ \begin{array}{l} C_{n,i} \\ D_{n,i} \end{array} \right\} \cos(\kappa_i z) \quad (13)$$

with the eigenvalues

$$\kappa_i = (2i - 1) \frac{\pi}{d}, \quad i = 1, \dots, \infty. \quad (14)$$

The  $C_{n,i}$  development coefficients are obtained by the projection of the magnetic polarization on the modes, namely

$$C_{n,i} = \begin{cases} \frac{1}{d} \int_0^{d/2} I_n(z) dz, & \text{for } i = 0 \\ \frac{2}{d} \int_0^{d/2} I_n(z) \cos(\kappa_i z) dz, & \text{for } i = 1, 2, \dots \end{cases} \quad (15)$$

The expansion coefficients for the magnetic induction  $D_{n,i}$  are determined by substituting (13) into (7), which yields

$$D_{n,i} = \begin{cases} 0, & \text{for } i = 0 \\ \frac{\kappa_i^2}{\kappa_i^2 + k_n^2} C_{n,i}, & \text{for } i = 1, 2, \dots \end{cases} \quad (16)$$

<sup>2</sup> It is a well known feature of magnetic materials that, owing to the symmetry of the B-H curve, only odd harmonics deliver a non-zero contribution to the solution. Nonetheless, numerical experimentation has revealed that taking also the even harmonics into account leads to slightly better results. This could be possibly explained by the fact that the actual B solution calculated at every iteration is not perfectly symmetric.

The general solution of (7) for the  $n$ -th harmonic is thus given by

$$B_n(z) = A_n \cosh(k_n z) + \sum_{i=1}^{\infty} \frac{\kappa_n^2}{\kappa_i^2 + k_n^2} C_{n,i} \cos(\kappa_i z). \quad (17)$$

Applying the boundary condition for the magnetic field at the upper surface of the plate to (17) and taking (8) into account, we obtain

$$\frac{1}{2} \mathcal{K}_0 \delta_{n,\pm 1} = \mu^{-1} \left[ A_n \cosh\left(\frac{k_n d}{2}\right) + C_{n,0} \right] \quad (18)$$

where  $\delta$  is the Kronecker's delta.

Therefore, the solution for the  $n$ -th harmonic of the magnetic field becomes at  $(l+1)$ th iteration

$$B_n^{(l+1)}(z) = \left[ \frac{\mu}{2} \mathcal{K}_0 \delta_{n,\pm 1} - C_{n,0}^{(l)} \right] \frac{\cosh(k_n z)}{\cosh(k_n d/2)} + \sum_{i=1}^{\infty} \frac{\kappa_n^2}{\kappa_i^2 + k_n^2} C_{n,i}^{(l)} \cos(\kappa_i z). \quad (19)$$

The first term of the sum gives the response of the linearized medium to the current, whereas the remaining two terms yield the contribution of the magnetic polarization. Note that the development coefficients for the magnetic polarization are calculated based on its value at the  $l$ th iteration, following the Picard-Banach scheme. The final expression in time domain will be obtained by summing the contributions of all harmonics according to (9).

### B. Pulsed excitation

Let us now consider a current described by an arbitrary pulse  $\mathcal{K}(t)$ . Our main tool here will be the Laplace transform  $F(s) = \mathcal{L}[f(t)]$ , defined by the integral pair

$$F(s) := \int_0^{\infty} f(t) e^{-st} dt \quad (20)$$

for the forward transform, and

$$f(t) = \frac{1}{2\pi i} \int_{Br} F(s) e^{st} ds \quad (21)$$

for the inverse transform, where  $Br$  stands for the Bromwich path of integration in the complex  $s$ -plane.

Taking the Laplace transform of (7) we obtain the inhomogeneous Helmholtz equation in the  $s$ -plane

$$\frac{\partial^2 B}{\partial z^2} - s\mu\sigma B = \frac{\partial^2 I}{\partial z^2}. \quad (22)$$

The solution of the homogeneous equation with account for the symmetry at  $z = 0$  reads

$$B^{(h)}(z, s) = A(s) \cosh(\sqrt{\mu\sigma s} z) \quad (23)$$

the coefficient  $A(s)$  being determined by the excitation waveform and the boundary conditions.

For the construction of the partial solution, we work as in the harmonic case, i.e. the spatial part of the magnetic field and the magnetic polarization is expanded in the eigenfunction basis

(13) yielding the following expressions for the development coefficients:

$$C_i(s) = \begin{cases} \frac{1}{d} \int_0^{d/2} I_n(z, s) dz, & \text{for } i = 0 \\ \frac{2}{d} \int_0^{d/2} I_n(z, s) \cos(\kappa_i z) dz, & \text{for } i = 1, 2, \dots \end{cases} \quad (24)$$

and

$$D_i(s) = \frac{1}{1 + s\tau_i} C_i(s) \quad (25)$$

with  $\tau_i = \mu\sigma/\kappa_i^2$ .

Application of the tangential magnetic field continuity across the plate surfaces yields

$$A(s) \cosh(\sqrt{\mu\sigma s} d/2) = \mu\mathcal{K}(s) + C_0(s) \quad (26)$$

which implies for the total solution of (22)

$$B(z, s) = [\mu\mathcal{K}(s) + C_0(s)] \frac{\cosh(\sqrt{sT} z/d)}{\cosh(\sqrt{sT}/2)} + \sum_{i=1}^{\infty} \frac{1}{1 + s\tau_i} C_i(s) \cos(\kappa_i z) \quad (27)$$

where we have set  $T := \mu\sigma d^2$ . Note that  $T$  is a measure of the system characteristic time [22].

The functional form of  $C_i(s)$  is arbitrary. Using the generalized pencil-of-function (GPOF) method [19], [20] though, we can approximate it via a weighted sum of rational functions, deduced by its dominant poles in the complex plane, namely

$$C_i(s) \approx \sum_{j=1}^{N_p} \frac{b_{ij}}{s - p_{ij}} \quad (28)$$

and (27) reduces to the more convenient form

$$B(z, s) = \left[ \mu\mathcal{K}(s) + \sum_{j=1}^{N_p} \frac{b_{0j}}{s - p_{0j}} \right] \frac{\cosh(\sqrt{sT} z/d)}{\cosh(\sqrt{sT}/2)} + \sum_{i=1}^{\infty} \frac{1}{1 + s\tau_i} \cos(\kappa_i z) \sum_{j=1}^{N_p} \frac{b_{ij}}{s - p_{ij}}. \quad (29)$$

It is convenient to consider the two contributions, namely that of the excitation current and the one from the magnetic polarization, separately, i.e. we write

$$B(z, s) = B_c(z, s) + B_p(z, s). \quad (30)$$

We shall work first with the second term since it is independent from the excitation. From inverse Laplace transform tables, we get the formula [23, (40), p. 259]

$$\mathcal{L}^{-1} \left[ \frac{1}{s - p} \frac{\cosh(x\sqrt{s})}{\cosh(l\sqrt{s})} \right] = \frac{\cosh(x\sqrt{p})}{\cosh(l\sqrt{p})} e^{pt} - y \left( \frac{x}{2l} \left| \frac{t}{l^2} \right| p l^2 \right) \quad (31)$$

where

$$y(v|\tau|\nu) := 2\pi \sum_{n=0}^{\infty} \frac{(n+1/2)(-1)^n \cos[(n+1/2)2\pi v]}{(n+1/2)^2 \pi^2 + \nu} \times e^{-(n+1/2)^2 \pi^2 \tau}. \quad (32)$$

Using (31),(32) as well as the standard formulas for the rational function transforms [23],  $B_p$  is transformed into the time domain - at the  $(l+1)$ th iteration - as follows

$$\begin{aligned} B_p^{(l+1)}(z, t) &= \sum_{j=1}^{N_p} b_{0j}^{(l)} \frac{\cosh(\sqrt{p_{0j} T} \hat{z})}{\cosh(\sqrt{p_{0j} T}/2)} e^{p_{0j} t} \\ &\quad - \sum_{j=1}^{N_p} b_{0j}^{(l)} y(\hat{z} | \frac{4t}{T} | p_{0j} T) \\ &\quad + \sum_{i=1}^{\infty} \sin(\kappa_i z) \sum_{j=1}^{N_p} b_{ij}^{(l)} \frac{e^{p_{ij} t} - e^{-t/\tau_i}}{1 + p_{ij} \tau_i} \end{aligned} \quad (33)$$

where  $\hat{z} := z/d$  stands for the normalized depth.

The time domain expression for the current response  $B_c$  depends on the excitation waveform, and it is not always amenable to a closed form. However, if we consider a step function excitation we arrive at a relatively simple expression for  $B_c$  using the inverse transform (31)

$$B_c(z, t) = \mu K_0 \left[ 1 - y\left(\hat{z} \left| \frac{4t}{T} \right| 0\right) \right]. \quad (34)$$

Perhaps a more elegant expression can be given in terms of the elliptic theta function. Recalling the transform [23, (37), p. 259],

$$\mathcal{L}^{-1} \left[ \frac{\cosh(x\sqrt{s})}{\cosh(l\sqrt{s})} \right] = -\frac{1}{l} \frac{\partial}{\partial x} \theta_1 \left( \frac{x}{2l} \left| \frac{\pi t}{l^2} \right. \right) \quad (35)$$

where  $-l \leq x \leq l$ , and  $\theta_1$  is the elliptic theta function defined as [23, pp. 387]

$$\theta_1(v|\tau) = (-\iota\tau)^{-1/2} \sum_{n=-\infty}^{\infty} (-1)^n e^{-\iota\pi(v-1/2+n)^2/\tau} \quad (36)$$

(34) is written as

$$B_c(z, t) = -\frac{1}{2} \mu K_0 \int_0^{t/T} \frac{\partial}{\partial \hat{z}} \theta_1(\hat{z} | \iota\pi\tau) d\tau. \quad (37)$$

Knowing the field response to a step current  $B_s$ , the respective response to an arbitrary excitation  $s$  can be easily obtained by utilizing the Duhamel's integral

$$B_c(z, t) = \frac{d}{dt} \int_0^t s(x) B_s(z, t-x) dx. \quad (38)$$

It is interesting to note that the current-related term of the plate response  $B_c$  for short times reduces to the corresponding solution for a half-space. This is not a surprising result since at sufficiently early times, the induced field at each side of the plate has not yet reached the opposite side, and the plate behaves as being of infinite thickness. The detailed proof is given in the appendix.

#### IV. 1D CYLINDRICAL PROBLEM: INFINITE SOLENOID

We move now to the cylindrical geometry by considering an infinite solenoid encircling an infinitely long ferromagnetic core. The geometry of the problem is illustrated in figure 2. The radius of the solenoid is  $\rho_a$  and the the number of turns per unit length is  $N$ . The core is assumed to be a cylindrical

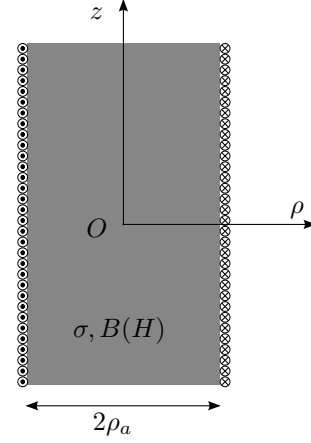


Fig. 2. Infinite solenoid with a ferromagnetic core.

rod of the same dimensions with the solenoid. The core material is considered to be again ferromagnetic with the same characteristics as the one examined above. The symmetry of the configuration results in a parallel to coil axis magnetic field ( $\mathbf{H} = H\mathbf{e}_z$ ) and an azimuthal electric field ( $\mathbf{E} = E\mathbf{e}_\phi$ ), and thus the magnetic constitutive relation will be again scalar, this time involving  $B_z, H_z$  and  $\hat{I}_z^3$ . The functional form of the constitutive equation will be given by (8).

The wave equation for the magnetic field in cylindrical coordinates reads

$$\frac{\partial^2 B}{\partial \rho^2} + \frac{1}{\rho} \frac{\partial B}{\partial \rho} - \mu\sigma \frac{\partial B}{\partial t} = \frac{\partial^2 \hat{I}}{\partial \rho^2} + \frac{1}{\rho} \frac{\partial \hat{I}}{\partial \rho}. \quad (39)$$

In the next sections we are going to consider separately the two time excitations that we also treated for the cartesian problem.

##### A. Harmonic excitation

The inhomogeneous Helmholtz equation for the  $n$ -th frequency reads

$$\frac{\partial^2 B_n}{\partial \rho^2} + \frac{1}{\rho} \frac{\partial B_n}{\partial \rho} - k_n^2 B_n = \frac{\partial^2 \hat{I}_n}{\partial \rho^2} + \frac{1}{\rho} \frac{\partial \hat{I}_n}{\partial \rho} \quad (40)$$

with the wavenumber

$$k_n^2 = \iota n \omega_0 \mu \sigma. \quad (41)$$

The solution of the homogeneous equation is given by the zero-order modified Bessel function

$$B_n^{(h)}(\rho) = A_n I_0(k_n \rho). \quad (42)$$

The eigenvalue equation of the spatial operator in (40) reads

$$\left[ \frac{\partial^2}{\partial \rho^2} + \frac{1}{\rho} \frac{\partial}{\partial \rho} \right] J_0(\kappa \rho) = -\kappa^2 J_0(\kappa \rho) \quad (43)$$

which form a complete basis in the cylindrical system with invariance along the azimuthal and the axial direction. Hence

<sup>3</sup>To avoid confusion with the modified Bessel function of the first kind, in the cylindrical problem the magnetic polarization will be distinguished by a hat.

the partial solution to (40) can be expanded to the following series

$$\begin{Bmatrix} \hat{I}_n(\rho) \\ B_n(\rho) \end{Bmatrix} = \begin{Bmatrix} C_{n,0} \\ D_{n,0} \end{Bmatrix} + \sum_{i=1}^{\infty} \begin{Bmatrix} C_{n,i} \\ D_{n,i} \end{Bmatrix} J_0(\kappa_i \rho) \quad (44)$$

with

$$J_0(\kappa_i \rho_a) = 0, \quad i = 0, 1, \dots, \infty. \quad (45)$$

The expansion coefficients for the magnetic polarization are calculated by the projections onto the basis functions, which for the cylindrical system yields

$$C_{n,i} = \begin{cases} \frac{2}{\rho_a^2} \int_0^{\rho_a} \rho \hat{I}_n(\rho) d\rho, & \text{for } i = 0 \\ \frac{2}{E_i^2} \int_0^{\rho_a} \rho J_0(\kappa_i \rho) \hat{I}_n(\rho, t) d\rho & \text{for } i = 1, 2, \dots \end{cases} \quad (46)$$

where  $E_i = \rho_a^2 J_1^2(\kappa_i \rho_a)$ .

The corresponding coefficients for the magnetic flux density  $D_{n,i}$  are related with  $C_{n,i}$  via the same relation used in the planar case (16).

Applying the boundary condition at the interface of the rod we obtain the value of the  $A_n$  coefficient

$$\mathcal{K}_0 \delta_{n,\pm 1} = \mu^{-1} [A_n I_0(k_n \rho_a) - C_{n,0}]. \quad (47)$$

The complete solution of the inhomogeneous cylindrical problem for the  $n$ -th harmonic can thus be written formally as follows:

$$\begin{aligned} B_n^{(l+1)}(\rho) = & \mu \mathcal{K}_0 \frac{I_0(k_0 \rho)}{I_0(k_0 \rho_a)} \delta_{n,\pm 1} + C_{n,0}^{(l)} \frac{I_0(k_n \rho)}{I_0(k_n \rho_a)} \\ & + \sum_{i=1}^{\infty} \frac{\kappa_n^2}{\kappa_i^2 + k_n^2} C_{n,i}^{(l)} J_0(\kappa_i \rho). \end{aligned} \quad (48)$$

Determining the expansion coefficients  $C_{n,i}$  for the unknown magnetization will yield the magnetic field distribution inside the solenoid.

### B. Pulsed excitation

Passing on the Laplace plane, as we did for the cartesian case, and following the same modal decomposition as above, we derive the field solution inside the rod for a given magnetic polarization

$$\begin{aligned} B(\rho, s) = & [\mu \mathcal{K}_0(s) + C_n(s)] \frac{I_0(\sqrt{sT} \hat{\rho})}{I_0(\sqrt{sT})} \\ & + \sum_{i=1}^{\infty} \frac{1}{1+s\tau_i} C_n(s) J_0(\kappa_i \rho) \end{aligned} \quad (49)$$

where this time the characteristic time of the system is given by  $T := \mu \sigma \rho_a^2$  and the normalized radius by  $\hat{\rho} := \rho / \rho_a$ . Decomposing again the coefficient expressions in terms of rational functions of their poles in the  $s$ -plane via the GPOF method, we obtain

$$\begin{aligned} B(\rho, s) = & \left[ \mu \mathcal{K}(s) + \sum_{j=1}^{N_p} \frac{b_{0j}}{s-p_{0j}} \right] \frac{I_0(\sqrt{sT} \hat{\rho})}{I_0(\sqrt{sT})} \\ & + \sum_{i=1}^{\infty} \frac{1}{1+s\tau_i} J_0(\kappa_i \rho) \sum_{j=1}^{N_p} \frac{b_{ij}}{s-p_{ij}}. \end{aligned} \quad (50)$$

To obtain the time domain solution we work as in the cartesian problem, i.e. we separate the current and the polarization contributions.

Let us consider first the inverse Laplace transform of the modified Bessel function ratio appearing in (50). In the lemma given in the appendix it is shown that

$$\mathcal{L}^{-1} \left[ \frac{I_n(\sqrt{sT} \hat{\rho})}{I_n(\sqrt{sT})} \right] = \frac{2}{T} \sum_{k=1}^{\infty} x_k \frac{I_n(x_k \hat{\rho})}{I_n'(x_k)} e^{x_k^2 t/T} \quad (51)$$

where  $x_k$  are the roots of the modified Bessel function  $I_0$ .

The above inverse Laplace transform is easily generalized to include a rational function as follows

$$\begin{aligned} \mathcal{L}^{-1} \left[ \frac{1}{s-a} \frac{I_0(\sqrt{sT} \hat{\rho})}{I_0(\sqrt{sT})} \right] \\ = \frac{2}{T} \sum_{k=1}^{\infty} x_k \frac{I_0(x_k \hat{\rho})}{I_0'(x_k)} e^{at} * e^{x_k^2 t/T} \end{aligned} \quad (52)$$

which taking into account the relation

$$e^{at} * e^{x_k^2 t/T} = \frac{e^{bt} - e^{at}}{b-a} \quad (53)$$

becomes

$$\mathcal{L}^{-1}[\dots] = 2 \sum_{k=1}^{\infty} x_k \frac{I_0(x_k \hat{\rho})}{I_0'(x_k)} \frac{e^{x_k^2 t/T} - e^{at}}{x_k^2 - aT} \quad (54)$$

Thus the inverse Laplace transform of the polarization contribution for the  $(l+1)$ th iteration yields

$$\begin{aligned} B_p^{(l+1)}(\rho, t) = & \frac{2}{T} \sum_{j=1}^{N_p} b_{0j}^{(l)} \sum_{k=1}^{\infty} x_k \frac{I_0(x_k \hat{\rho})}{I_0'(x_k)} \frac{e^{x_k^2 t/T} - e^{p_{0j} t}}{x_k^2 - p_{0j} T} \\ & + \sum_{i=1}^{\infty} J_0(\kappa_i \rho) \sum_{j=1}^{N_p} b_{ij}^{(l)} \frac{e^{p_{ij} t} - e^{-t/\tau_i}}{1 + p_{ij} \tau_i} \end{aligned} \quad (55)$$

It is perhaps interesting to note that the zeros of Bessel functions are involved both in the spatial ( $\kappa_i \rho_a$ ) and temporal ( $x_k$ ) expansions.

The response to the step current excitation is a special case of (54) with  $a=0$ :

$$B_s(\rho, t) = 2\mu \mathcal{K}_0 \sum_{k=1}^{\infty} \frac{I_0(x_k \hat{\rho})}{I_0'(x_k)} \frac{e^{x_k^2 t/T} - 1}{x_k} \quad (56)$$

and the response to an arbitrary input waveform will be obtained again by the Duhamel's integral (38).

## V. RESULTS

The modal solution has been compared with numerical results obtained using a two-dimensional numerical code based on the FIT method. The numerical solution is obtained by direct integration in the time domain using a two-step backward differentiation implicit Euler scheme [24].

We consider first the configuration of figure 1. The plate thickness is 5 mm and the material is taken to be 1010 carbon steel with conductivity equal to 6.993 MS/m. When working with non-linear material laws it is more convenient to use approximate parametric models that directly fit the experimental data. The Fröhlich-Kennelly relation offers such a simple yet adequate approximation of the measured non-linear curve,

when hysteresis effects are neglected. The Fröhlich-Kennelly approximation reads as

$$B = \frac{H}{\alpha + \beta|H|} \quad (57)$$

with  $\alpha$  and  $\beta$  free parameters chosen to best fit the experimental data. The estimated values obtained by the fitting procedure for the given steel grade are  $\alpha = 206.42$  and  $\beta = 0.59148$ . The parametric approximation of the material curve is shown in figure 3.

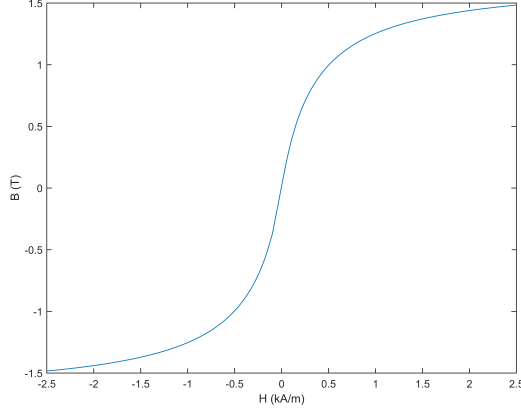


Fig. 3. Approximated B-H curve of the 1010 steel.

The non-linear problem has been solved using the two excitations considered above, namely a sinusoidal current at 50 Hz and a step function. The density of the current layer is taken equal to 1.5 kA/m for both cases, which lies far beyond the linear region as one can see from figure 3.

Figure 4a shows the field variation as a function of the depth at the peak of the input. The modal solution is compared with the numerical one obtained with the FIT solver [24]. The temporal variation of the magnetic field at a fixed point 25  $\mu\text{m}$  underneath the plate surface is depicted in figure 4b. To get a picture of the harmonic distortion due to the non-linearity of the material, a harmonic signal of the same amplitude is superposed to the field response.

The transient field response to a step excitation is shown in figure 5a,b. The field profile is given 10 ms after the switching of the current. The field signal is given at the same location as in figure 4.

The number of modes taken into account in both calculations (with harmonic and step excitation) was 150. The frequency spectrum considered for treatment of the harmonic excitation was truncated to the 13th harmonic. As far as the step-function response is concerned, 5 poles were proved sufficient to obtain the demonstrated results precision. The computational time for the solution of the two problems was 4.2 s and 31 s respectively, which has to be compared with the 73 s and 31 s that takes the numerical solution of the same problems using the FIT transient solver.

The second configuration we consider is the one of the solenoid with the iron core depicted in figure 2. The core diameter is 15.875 mm and consists of the same material as the

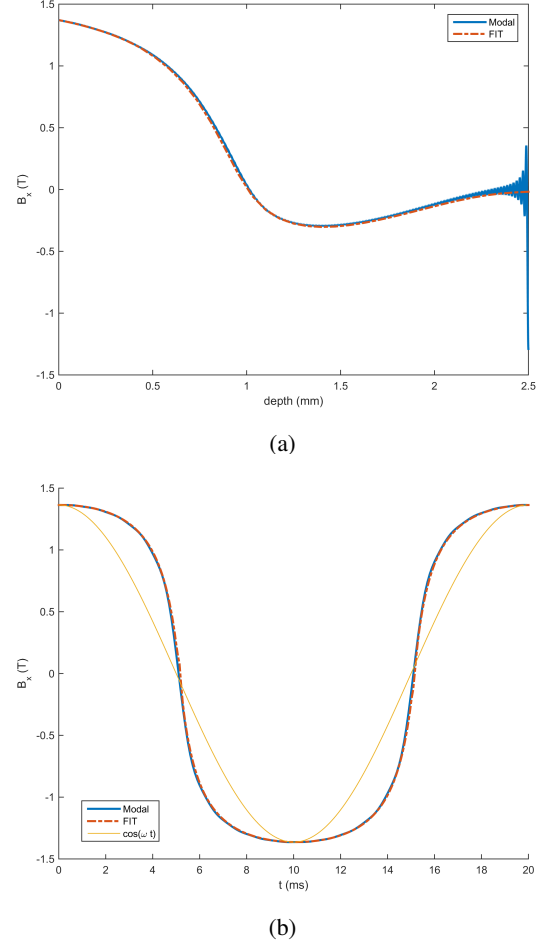


Fig. 4. Analytical vs. numerical solution for the magnetic flux density in a ferromagnetic plate with harmonic excitation: (a) field profile as a function of depth, (b) time signal at 25  $\mu\text{m}$  depth. A harmonic signal of equal amplitude is also drawn to illustrate the distortion due to the non-linearity.

plate (1010 steel). Figure 6 give the field profile and the time signal for a harmonic excitation at 50 Hz, whereas figure 7 depicts the corresponding solution for step excitation. The field signal in both cases is given at a depth equal to one third of the rod diameter. The field snapshots are obtained at the peak of the excitation and at 20 ms respectively.

The number of modes considered for the semi-analytical solver was 150 for the harmonic excitation and 300 for the step excitation. The number of harmonics taken into account for the cosinusoidal excitation was 20, and 12 poles were used for the GPOF decomposition of the transient problem. The computational times for the modal solution of the two excitations were 21 s and 70 s using the modal solver, which are clearly lower than the 1205 s and 228 s of the numerical solution.

A general remark that can be made after the comparison of the above computational times is that the numerical solution is slower for all the examined cases except for the infinite plate with the step excitation, where the two solvers demonstrate the same performances.

In all cases a very satisfactory agreement between the modal and the numerical solution is obtained apart from a number

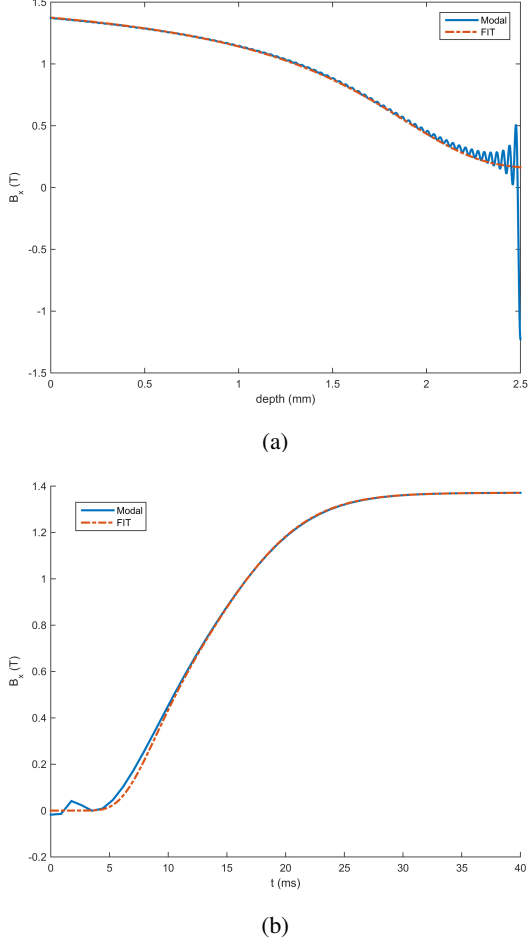


Fig. 5. Analytical vs. numerical solution for the magnetic flux density in a ferromagnetic plate excited by a step function: (a) field profile as a function of depth, (b) time signal at 25  $\mu\text{m}$  depth.

of artificial oscillations due to the Gibbs effect.

## VI. SUMMARY

The Picard-Banach iterative scheme has been combined with a modal approach for the solution of the non-linear induction problem in ferromagnetic specimens. For harmonic excitations, the enriched spectrum of the higher harmonics is treated by means of Fourier series, whereas the transient response to a general pulsed excitation is obtained by applying the Laplace transform. The main complication when working in the Laplace domain is the calculation of the inverse transforms, which for arbitrary signals has to be done numerically. In this work, an alternative approach based on the GPOF algorithm for the signal decomposition in exponential functions is used, allowing the calculation of the inverse transform via the superposition of closed-form transients.

The present analysis is a first step towards the semi-analytical treatment of non-linear problems, and outlines the method that will be employed for the treatment of more realistic two and three-dimensional problems. The interest in applying modal solutions rather than generic numerical tools lies on the evasion of domain meshing and the reduced computational times.

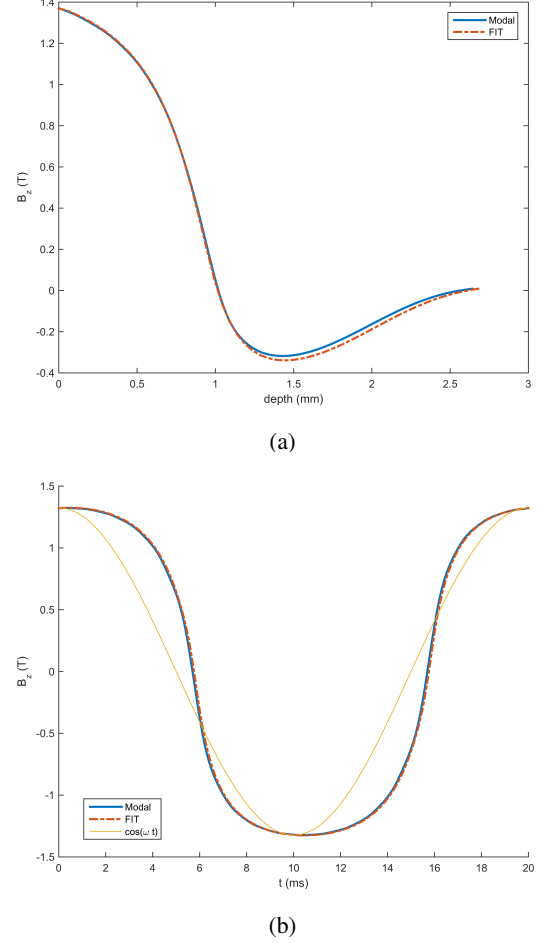


Fig. 6. Analytical vs. numerical solution for the magnetic flux density in a ferromagnetic rod with harmonic excitation. (a) Field profile as a function of depth, (b) field temporal variation.

## VII. ACKNOWLEDGEMENT

This work is supported by the CIVAMONT project, aiming at developing scientific collaborations around the NDT simulation platform CIVA developed at CEA LIST.

## APPENDIX A

### ASYMPTOTIC BEHAVIOUR FOR SHORT TIME

To study the asymptotic behaviour of the solution for short time, we shall consider the field response to an exponential pulse (second term of the bracketed expression in (29)). The unit step response (first term in the bracket) can be considered as a special case of the former with zero pole  $p = 0$ . Thus, let us return to the inverse Laplace transform of (35) and let us express it as a convolution integral

$$\begin{aligned} s(t) &:= \mathcal{L}^{-1} \left[ \frac{1}{s-p} \frac{\cosh(x\sqrt{s})}{\cosh(l\sqrt{s})} \right] \\ &= -\frac{1}{t} e^{pt} * \frac{\partial}{\partial x} \theta_1 \left( \frac{x}{2l} \middle| \frac{i\pi t}{l^2} \right) \end{aligned} \quad (58)$$

where it was made use of (35). The last relation can also be written

$$s(t) = -\frac{1}{2l^2} e^{pt} * \frac{\partial}{\partial v} [\theta_1(v|\tau)]_{v=x/2l, \tau=i\pi t/l^2} \quad (59)$$



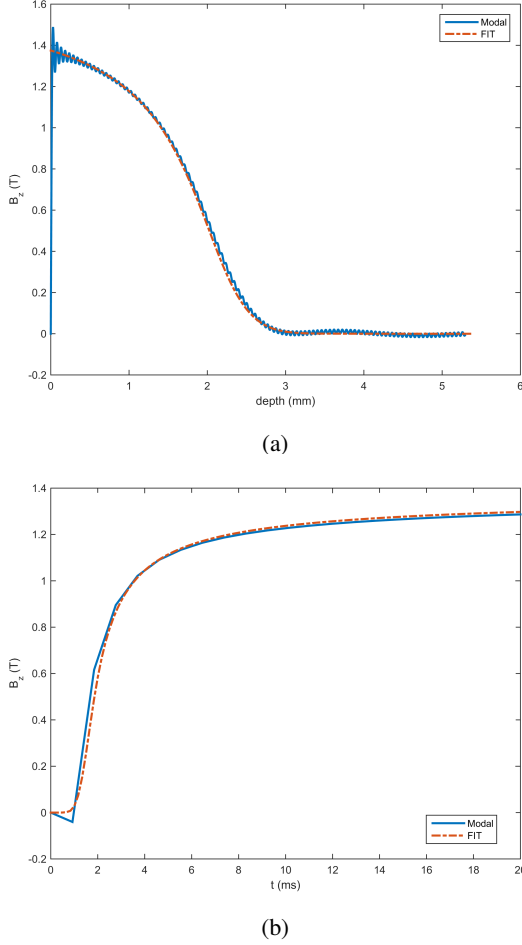


Fig. 7. Analytical vs. numerical solution for the magnetic flux density in a ferromagnetic rod with harmonic excitation. (a) Field profile as a function of depth, (b) field temporal variation.

We calculate the derivative of the elliptic theta function making use of its definition (36)

$$\begin{aligned} \frac{\partial}{\partial v} \theta_1(v|\tau) &= (-\iota\tau)^{-1/2} \sum_{n=-\infty}^{\infty} (-1)^n e^{-\iota\pi(v-1/2+n)^2/\tau} \\ &= (-\iota)^{1/2} 2\pi\tau^{-3/2} \sum_{n=-\infty}^{\infty} (-1)^n (v-1/2+n) \\ &\quad \times e^{-\iota\pi(v-1/2+n)^2/\tau} \end{aligned} \quad (60)$$

and we substitute in (59), which becomes after some simplifications

$$s(t) = \frac{l}{2\sqrt{\pi}} \sum_{n=-\infty}^{\infty} (-1)^n \left(\frac{x}{l} - 1 + 2n\right) e^{pt} * t^{-3/2} \times e^{-(x/l-1+2n)^2 l^2 / 4t}. \quad (61)$$

Now let us calculate the convolution integral

$$\begin{aligned} I_n(t|a) &= \int_0^t e^{p(t-\tau)} \tau^{-3/2} e^{-a/\tau} d\tau \\ &= e^{pt} \int_0^t e^{-p\tau} \left[ \frac{d}{d\tau} \int_0^{\tau} u^{-3/2} e^{-a/u} du \right] d\tau. \end{aligned} \quad (62)$$

With the change of variable  $\xi = \sqrt{a/u}$  the interior integral becomes

$$\int_0^{\tau} u^{-3/2} e^{-a/u} du = \sqrt{\frac{\pi}{a}} \operatorname{erfc}\left(\sqrt{\frac{a}{\tau}}\right) \quad (63)$$

whence

$$I_n(t|a) = \sqrt{\frac{\pi}{a}} e^{pt} \int_0^t e^{-p\tau} \frac{d}{d\tau} \operatorname{erfc}\left(\sqrt{\frac{a}{\tau}}\right) d\tau \quad (64)$$

and applying integration by parts

$$\begin{aligned} I_n(t|a) &= \sqrt{\frac{\pi}{a}} e^{pt} \left[ e^{-p\tau} \operatorname{erfc}\left(\sqrt{\frac{a}{\tau}}\right) \right]_0^t \\ &\quad + \sqrt{\frac{\pi}{a}} p e^{pt} \int_0^t e^{-p\tau} \operatorname{erfc}\left(\sqrt{\frac{a}{\tau}}\right) d\tau. \end{aligned} \quad (65)$$

The integral in the right hand side exists in closed form [25, 7.4.37]

$$\begin{aligned} \int e^{-p\tau} \operatorname{erfc}\left(\sqrt{\frac{a}{\tau}}\right) d\tau &= -\frac{1}{p} \left\{ e^{-p\tau} \operatorname{erfc}\left(\sqrt{\frac{a}{\tau}}\right) \right. \\ &\quad + \frac{1}{2} e^{-p\tau-a/\tau} \left[ w(\sqrt{-p\tau} + \iota\sqrt{\frac{a}{\tau}}) \right. \\ &\quad \left. \left. + w(-\sqrt{-p\tau} + \iota\sqrt{\frac{a}{\tau}}) \right] \right\} + \text{const} \end{aligned} \quad (66)$$

where  $w(z) = e^{-z^2} \operatorname{erfc}(-\iota z)$ . Hence

$$\begin{aligned} \int e^{-p\tau} \operatorname{erfc}\left(\sqrt{\frac{a}{\tau}}\right) d\tau &= -\frac{e^{-p\tau}}{p} \operatorname{erfc}\left(\sqrt{\frac{a}{\tau}}\right) \\ &\quad + \frac{1}{2p} \left[ e^{2\sqrt{pa}} \operatorname{erfc}(\sqrt{p\tau} + \sqrt{\frac{a}{\tau}}) \right. \\ &\quad \left. + e^{-2\sqrt{pa}} \operatorname{erfc}(-\sqrt{p\tau} + \sqrt{\frac{a}{\tau}}) \right] \end{aligned} \quad (67)$$

where the integration constant is implied. Substituting in (65) and taking into account  $\lim_{z \rightarrow \infty} \operatorname{erfc}(z) = 0$  we obtain

$$\begin{aligned} I_n(t|a) &= \sqrt{\frac{\pi}{a}} \frac{e^{pt}}{2} \left[ e^{2\sqrt{pa}} \operatorname{erfc}(\sqrt{pt} + \sqrt{\frac{a}{t}}) \right. \\ &\quad \left. + e^{-2\sqrt{pa}} \operatorname{erfc}(-\sqrt{pt} + \sqrt{\frac{a}{t}}) \right]. \end{aligned} \quad (68)$$

Equation (61) can thus be written as

$$\begin{aligned} s(t) &= \frac{l}{2\sqrt{\pi}} \sum_{n=-\infty}^{\infty} (-1)^n \left(\frac{x}{l} - 1 + 2n\right) \\ &\quad \times I_n \left[ t \left| \left(\frac{x-l}{2} + nl\right)^2 \right| \right] \end{aligned} \quad (69)$$

i.e. we have expressed the inverse Laplace transform as an infinite series of complementary error functions.

Particular interest presents the short time limit, i.e.  $t \rightarrow 0$ . The series of (69) is a rapidly converging series, which means that for small  $t$  (or equivalently for large complementary error function arguments) we can consider only the zero term ( $n = 0$ ):

$$s(t) \approx \frac{1}{2\sqrt{\pi}} (x-l) I_n \left[ t \left| \frac{(x-l)^2}{4} \right| \right] \quad (70)$$

which substituting (68) and setting  $x \rightarrow \sqrt{T}\hat{z}$ ,  $l \rightarrow \sqrt{T}/2^4$  yields

$$\begin{aligned} s(t) &\approx \frac{e^{pt}}{2} \left[ e^{\sqrt{pT}(1/2-\hat{z})} \operatorname{erfc}\left(\sqrt{\frac{T}{4t}}(1/2-\hat{z}) + \sqrt{pt}\right) \right. \\ &\quad \left. + e^{-\sqrt{pT}(1/2-\hat{z})} \operatorname{erfc}\left(\sqrt{\frac{T}{4t}}(1/2-\hat{z}) - \sqrt{pt}\right) \right]. \end{aligned} \quad (71)$$

<sup>4</sup>Only the positive sign of the quantity  $x-l$  has physical meaning.

Now let us consider the field response to an exponential signal  $e^{pt}$  in a half-space. The response in the Laplace domain is given by the relation

$$B_e(z, s) \sim \frac{e^{-\sqrt{s\sigma\mu}(d/2-z)}}{s-p} = \frac{e^{-\sqrt{sT}(1/2-\hat{z})}}{s-p} \quad (72)$$

which recalling the transform [23, (10), p. 246] is inverted into the time domain as follows

$$B_e(z, t) \sim \frac{e^{pt}}{2} \left[ e^{\sqrt{pT}(1/2-\hat{z})} \operatorname{erfc}\left(\sqrt{\frac{T}{4t}}(1/2-\hat{z}) + \sqrt{pt}\right) + e^{-\sqrt{pT}(1/2-\hat{z})} \operatorname{erfc}\left(\sqrt{\frac{T}{4t}}(1/2-\hat{z}) - \sqrt{pt}\right) \right] \quad (73)$$

which is identical with (71). In other words the plate response for short time reduces to the one of the half-space. From the point of physical interpretation, this means that at sufficiently short time, the eddy-current field has not yet reached the  $z = -d/2$  boundary, and therefore the plate is equivalent to a half-space.

#### APPENDIX B DERIVATION OF (51)

We seek the inverse Laplace transform of the complex function

$$F(s) = \frac{I_n(\sqrt{sT}\hat{\rho})}{I_n(\sqrt{sT})}. \quad (74)$$

This transform is not found in the most standard inverse transform tables.

To examine the behaviour of  $F(s)$  in the  $\operatorname{Re}[s] > 0$  half-plane for  $s \rightarrow \infty$ , we consider the asymptotic form of the modified Bessel functions

$$\frac{I_n(\sqrt{sT}\hat{\rho})}{I_n(\sqrt{sT})} \sim \exp\left[\sqrt{sT}(\hat{\rho}-1)\right] / \sqrt{\hat{\rho}} \quad (75)$$

for  $|\arg| < \pi/2$ , which is analytic and vanishes at  $s \rightarrow \infty$  for every  $\hat{\rho} < 1$ . Hence  $F(s)$  is analytic and  $\lim_{z \rightarrow \infty} F(s) = 0$ , bounded in the  $\operatorname{Re}[s] > 0$  half-plane except for the zeros of the Bessel function in the denominator, and the inverse Laplace transform exists. For  $\hat{\rho} = 1$ ,  $F(s) = 1$ , and its inverse transform is the Dirac delta function.

Let us consider  $\hat{\rho} < 1$ . Using a basic result of the complex analysis (known as complex inversion formula [26]) the inverse Laplace transform of the function  $F(s)$  can be written as

$$f(t) = \sum_{k=1}^{\infty} \operatorname{Res}[F(s)e^{st}]_{s=s_k} \quad (76)$$

where  $\operatorname{Res}[F(s)e^{st}]$  are the residues of  $F(s)e^{st}$ . Substituting the considered transformed function (51) into (76), we obtain

$$\begin{aligned} \mathcal{L}^{-1}\left[\frac{I_n(\sqrt{sT}\hat{\rho})}{I_n(\sqrt{sT})}\right] &= \sum_{k=1}^{\infty} \frac{I_n(\sqrt{s_k T}\hat{\rho})}{\frac{\partial I_n(\sqrt{s_k T})}{\partial s}} e^{s_k t} \\ &= \frac{1}{2\sqrt{T}} \sum_{k=1}^{\infty} \sqrt{s_k} \frac{I_n(\sqrt{s_k T}\hat{\rho})}{I_n'(\sqrt{s_k T})} e^{s_k t} \end{aligned} \quad (77)$$

where  $s_k$  is related to the Bessel function zeros  $x_k$  via  $\sqrt{s_k T} = x_k$ . Equation (77) thus becomes

$$\mathcal{L}^{-1}[\dots] = \frac{2}{T} \sum_{k=1}^{\infty} x_k \frac{I_n(x_k \hat{\rho})}{I_n'(x_k)} e^{x_k^2 t/T} \quad (78)$$

which is the sought relation.

#### REFERENCES

- [1] I. Munteanu, S. Drobny, T. Weiland, and D. Ioan, "Triangle search method for nonlinear electromagnetic field computation," *COMPEL*, vol. 20, no. 2, pp. 417–430, 2001.
- [2] R. Albanese and G. Rubinacci, "Numerical procedures for the solution of nonlinear electromagnetic problems," *IEEE Trans. Magn.*, vol. 28, no. 2, pp. 1228–1231, Mar. 1992.
- [3] O. B  r   and K. Preis, "An efficient time domain method for nonlinear periodic eddy current problems," *IEEE Trans. Magn.*, vol. 42, no. 4, pp. 695–698, Apr. 2006.
- [4] S. Drobny and T. Weiland, "Numerical calculation of nonlinear transient field problems with the newton-raphson method," *IEEE Trans. Magn.*, vol. 36, no. 4, pp. 809–812, Jul. 2000.
- [5] R. Albanese, F. I. Hantila, and G. Rubinacci, "A nonlinear eddy current integral formulation in terms of a two-component current density vector potential," *IEEE Trans. Magn.*, vol. 32, no. 3, pp. 784–787, May 1996.
- [6] I. R. Circ and F. Hantila, "An efficient harmonic method for solving nonlinear time-periodic eddy-current problems," *IEEE Trans. Magn.*, vol. 42, no. 4, pp. 695–698, Apr. 2006.
- [7] W. Wolman and H. Kaden, "  ber die Wirbelstromverz  gerung magnetischer Schaltvorg  nge," *Z. Techn. Phys.*, vol. 13, no. 7, pp. 330–335, Jul. 1932.
- [8] W. MacLean, "Theory of strong electromagnetic waves in massive iron," *J. Appl. Phys.*, vol. 25, no. 10, pp. 1267–1270, Oct. 1954.
- [9] A. Papoulis, "Penetration of an electromagnetic wave into a ferromagnetic material," *J. Appl. Phys.*, vol. 25, no. 2, pp. 169–176, Feb. 1954.
- [10] A. H. Nayfeh and O. R. Asfar, "An analytical solution of the nonlinear eddy-current losses in ferromagnetic materials," *IEEE Trans. Magn.*, vol. 10, no. 2, pp. 327–331, Jun. 1974.
- [11] D. Labridis and P. Dokopoulos, "Calculation of eddy current losses in nonlinear ferromagnetic materials," *IEEE Trans. Magn.*, vol. 25, no. 3, pp. 2665–2669, May 1989.
- [12] S. K. Burke and T. P. Theodoulidis, "Impedance of a horizontal coil in a borehole: a model for eddy-current borehole probes," *J. Phys. D: Appl. Phys.*, vol. 37, pp. 485–494, 2004.
- [13] J. R. Bowler and T. P. Theodoulidis, "Eddy currents induced in a conducting rod of finite length by a coaxial encircling coil," *J. Phys. D: Appl. Phys.*, vol. 38, no. 16, pp. 2861–2868, Aug. 2005.
- [14] T. P. Theodoulidis and J. R. Bowler, "Eddy current coil interaction with a right-angled conductive wedge," *Proc. R. Soc. London, Ser. A*, vol. 461, no. 2062, pp. 3123–3139, Oct. 2005.
- [15] —, "Impedance of an induction coil at the opening of a borehole in a conductor," *J. Appl. Phys.*, vol. 103, no. 2, pp. 024 905–1–024 905–9, Jan. 2008.
- [16] A. Skarlatos and T. Theodoulidis, "Solution to the eddy-current induction problem in a conducting half-space with a vertical cylindrical borehole," *Proc. R. Soc. London, Ser. A*, vol. 468, no. 2142, pp. 1758–1777, Jun. 2012.
- [17] J. Bowler and M. Johnson, "Pulsed eddy-current response to a conducting half-space," *IEEE Trans. Magn.*, vol. 33, no. 3, pp. 2258–2264, May 1997.
- [18] F. Fu and J. Bowler, "Transient eddy-current driver pickup probe response due to a conductive plate," *IEEE Trans. Magn.*, vol. 42, no. 8, pp. 2029–2037, Aug. 2006.
- [19] V. K. Jain, T. K. Sarkar, and D. D. Weiner, "Rational modeling by pencil-of-functions method," *IEEE Trans. Acoust., Speech, Signal Process.*, vol. 31, no. 3, pp. 564–573, Jun. 1983.
- [20] Y. Hua and T. K. Sarkar, "Generalized pencil-of-function method for extracting poles of an EM system from its transient response," *IEEE Trans. Antennas Propag.*, vol. 37, no. 2, pp. 229–234, Feb. 1989.
- [21] F. I. H  n  il  , "A method of solving stationary magnetic field in non-linear media," *Rev. Roum. Sci. Tech.-  lectrotechn. et   nerg.*, vol. 20, no. 3, pp. 397–407, 1975.
- [22] J. D. Jackson, *Classical electrodynamics*, 3rd ed.
- [23] A. Erd  lyi, Ed., *Tables of Integral Transforms*. New York: McGraw-Hill, 1954, vol. 1.

- [24] M. C. M. Wilke and T. Weiland, "Extrapolation strategies in transient magnetic field simulations," *IEEE Trans. Magn.*, vol. 39, no. 3, pp. 1171–1174, May 2003.
- [25] M. Abramowitz and I. Stegun, *Handbook of Mathematical Functions with Formulas, Graphs, and Mathematical Tables*. New York: Dover, 1972.
- [26] J. E. Marsden, *Basic Complex Analysis*. New York: W. H. Freeman, 1999.